Optical evidence for blue shift in topological insulator bismuth selenide in the few-layer limit

Yub Raj Sapkota, Asma Alkabsh, Aaron Walber, Hassana Samassekou, and Dipanjan Mazumdar

Citation: Appl. Phys. Lett. **110**, 181901 (2017); doi: 10.1063/1.4982631
View online: http://dx.doi.org/10.1063/1.4982631
View Table of Contents: http://aip.scitation.org/toc/apl/110/18
Published by the American Institute of Physics

Optical evidence for blue shift in topological insulator bismuth selenide in the few-layer limit

Yub Raj Sapkota,[1] Asma Alkabsh,[1] Aaron Walber,[1] Hassana Samassekou,[1] and Dipanjan Mazumdar[1,2]
[1]*Department of Physics, Southern Illinois University, Carbondale, Illinois 62901, USA*
[2]*Materials Technology Center, Southern Illinois University, Carbondale, Illinois 62901, USA*

(Received 25 February 2017; accepted 13 April 2017; published online 1 May 2017)

Optical bandgap properties of high-quality few-layer topological insulator Bi_2Se_3 thin films are investigated using broadband absorption spectroscopy. We provide direct optical evidence for blue shift in the bulk bandgap of Bi_2Se_3 as it approaches the two-dimensional limit. The blue shift is robust and observed in both protected (capped) and exposed (uncapped) thin films. The behavior is strongest below six quintuple layers (QLs), particularly at the 2 and 3 QL level, where finite-size effects are known to be most significant in Bi_2Se_3. A further bandgap increase is observed in all films that we attribute to the Burstein-Moss effect. Our result provides additional insights into the scaling behavior of topological materials. The bandgap increase has a significant impact on the electronic and optoelectronic applications of topological insulators. *Published by AIP Publishing.* [http://dx.doi.org/10.1063/1.4982631]

Topological insulators (TIs) have gained much attention in basic and applied physics research due to the existence of "topologically protected" gapless surface states.[1–3] Such quantum states are immune to non-magnetic impurities as the electron momentum remains locked to its spin.[4] The room temperature discovery of the protected states in real materials with a strong spin-orbit coupling (such as BiSb, Bi_2Se_3, and Sb_2Te_3) without the application of an external magnetic field is also interesting for device applications in spintronics and fault-tolerant quantum computing.[5–10]

Bi_2Se_3 is a prototypical example among 3D Topological insulators.[4] A single Dirac cone was observed at the Γ point in bulk Bi_2Se_3 using angle-resolved photoemission spectroscopy (ARPES)[3,11,12] and scanning tunneling microscopy measurements.[13] It is classified as a strong topological insulator,[14] where the surface states retain zero-gap despite the presence of atomic-level non-magnetic impurities. The literature on Bi_2Se_3 thin films is also growing. Recent experiments demonstrated proximity-induced superconductivity[15,16] and ferromagnetism,[5] both phenomena associated with symmetry breaking. Exotic effects such as the Quantum anomalous Hall effect are also reported at ultralow temperatures.[17–19]

Many applications of TIs such as Bi_2Se_3 will rely on their scaling behavior. It is, therefore, important and intriguing to ask as to what happens to such exotic materials as they approach the two-dimensional limit? Thin films provide an ideal platform to investigate such topics. One of the more intriguing consequences of finite-size effects in TIs is the opening of an energy gap in the surface states.[20–24] Experimentally, this was directly verified by Zhang *et al.*[25] and Sakamoto *et al.*[26] in ultra-thin Bi_2Se_3 films. The gap opening is substantially large (∼few tenths of eV). Weak localization effects also produce a gap opening in few-layer Bi_2Se_3, but it is of the order of meV.[27,28] Also, recently, Vargas *et al.* reported a large blue shift in Bi_2Se_3 nanoparticles, which they attributed to quantum-confinement effects in all directions.[29] All these reports demonstrate that finite-size can have a profound impact on topological materials. In this work, we report that bulk optical bandgap changes also occur in such materials in the 2-dimensional limit.

Investigation of optical properties of Bi_2Se_3 thin films has been a subject of previous studies. Variation of bulk bandgap with thickness has also been noted. Post *et al.*[30] studied uncapped 15–99 quintuple layer (QL) Bi_2Se_3 films and found bandgap values below 0.3 eV that are attributed to impurity states or surface contamination. Eddrief *et al.*[31] measured the optical properties of 3–54 QL Bi_2Se_3 thin films. While they cover a broad thickness range, the optical properties of the 3 QL film do show a behavior that is consistent, but not clearly reported, with an increase in the bandgap. Higher optical transmittance in 5 or 6 QL Bi_2Se_3 films has been reported that implies a higher bandgap.[32,33] However, a systematic bulk bandgap investigation is lacking at the two-dimensional (few-layer) limit of Bi_2Se_3.

Here, we report the optical properties of few-layer Bi_2Se_3 (∼2–10 QL) thin films. High-quality Bi_2Se_3 films (both capped and uncapped) were grown on Si/SiO_2 and quartz substrates using radio frequency magnetron sputtering. We have discovered up to 0.5 eV increase in the bulk bandgap of Bi_2Se_3 as the thickness is reduced to 2 QL. We explain the blue shift as due to a combination of bulk electronic structure changes at lower dimensions and Burstein-Moss (BM) effect. The blue shift is robust and observed in samples with and without a protective capping layer. Our work consolidates a growing number of studies that highlight finite-size effects in topological materials.

In this work, high-quality Bi_2Se_3 few-layer thin films were fabricated in the 2–10 nm thickness range that roughly translates to 2–10 quintuple layers (1 QL ∼0.95 nm). Bi_2Se_3 was grown using a commercially available stoichiometric target, and sputtered in a high vacuum magnetron sputtering system (base pressure 4×10^{-9} Torr). Bi_2Se_3 films were grown at room temperature and annealed *in-situ* at 300 °C. We recently employed a similar method to grow other large-

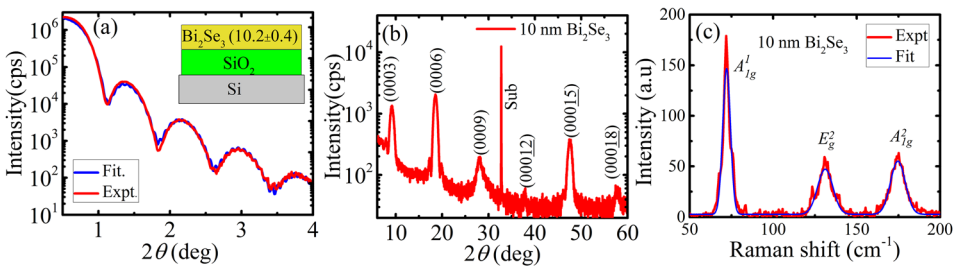

FIG. 1. (a) High-resolution X-ray reflectivity of the ~10 nm Bi_2Se_3 thin film grown on Si/SiO_2 substrate. The inset shows the thickness and roughness value of the Bi_2Se_3 film as obtained from the fit of reflectivity data. (b) The X-ray diffraction pattern of the 10 nm Bi_2Se_3 film showing only (000l) peaks, implying out-of-plane growth. (c) Raman vibration modes of the Bi_2Se_3 film showing the characteristic $A^1{}_1g$, E^2g, and $A^2{}_1g$ modes.

area layered materials such as MoS_2.[34] The films were grown on Si/SiO_2(100 nm) substrates for the X-ray, Raman, and ellipsometry analysis, and on transparent quartz substrates for the absorption spectroscopy study. To protect the surface from contamination and oxidation and yet retain optical transparency at the infrared and visible wavelengths, some Bi_2Se_3 thin films were capped with an amorphous BN layer grown *in-situ* at room temperature.

Structural and interface properties were characterized by high-resolution X-ray diffraction (XRD) and reflectivity (XRR) using a Rigaku Smartlab Diffractometer equipped with a Ge (220) monochromator to obtain Cu $K\alpha_1$ radiation. Raman spectroscopy was employed to confirm the vibrational modes of Bi_2Se_3 using a Nanophoton Raman-11 with a 532 nm laser. The laser power was kept low at 10 mW to avoid local heating. Optical constants such as complex dielectric constants (ε_1,ε_2) were investigated using a spectroscopic ellipsometer (JA Wollam M2000V, 1.1–3.0 eV), and the optical bandgap was measured using a broadband optical spectrometer (Shimadzu UV-3600 Plus) in the 0.375–6.2 eV range. Hall measurements were done using a NanoMagnetics Instruments ezHEMS system.

Figure 1 shows the structural characteristics of an uncapped 10 nm Bi_2Se_3 thin film grown on Si/SiO_2 substrate. In Fig. 1(a), we show the X-ray reflectivity (XRR) data of the film. The oscillatory thickness pattern of the ~10 nm Bi_2Se_3 layer and the 100 nm SiO_2 layer is observed. This is indicative of sharp interfaces. The thickness and roughness values as obtained from the reflectivity fit[35,36] are shown in the inset of Fig. 1(a). A roughness of ~0.4 nm is less than half a quintuple layer. The extracted density of the Bi_2Se_3 film is also in very good agreement with the bulk value. Fig. 1(b) shows the high-resolution theta-2theta X-ray diffraction (XRD) pattern of the 10 QL Bi_2Se_3 film. Clear diffraction peaks are identified for the (002) silicon substrate (labeled as "sub") and (000*l*) peaks of Bi_2Se_3. This is indicative of out-of-plane growth. Thickness fringes are also observed around the (0003) and (0006) peaks, which imply very smooth films. Off-axis measurements on high Miller indices peaks gave a = 4.17 Å, c = 28.56 Å. The XRR and XRD data of the 6 QL film are shown in Fig. S1 (see supplementary material). Taken together, we confirm that the properties of few-layer Bi_2Se_3 films are of superior bulk and interface quality. Additional crystalline structure characterization was also performed using Raman spectroscopy. The raw data and the line shape fits are shown in Fig. 1(c). Clear Raman modes were observed at ~72.0 cm^{-1}, 131.1 cm^{-1}, and 174.6 cm^{-1} which correspond to $A^1{}_1g$, E^2g, and $A^1{}_2g$ modes of Bi_2Se_3.[37] The full width at half maximum is ~5 cm^{-1} for the $A^1{}_1g$ mode and ~9–10 cm^{-1} for both the E^2g and $A^1{}_2g$ modes. These values are comparable to few-layer single crystals[37] and reiterates the high crystalline quality of the films.

We now discuss spectroscopic ellipsometry investigations performed in the spectral range of 1.1–3.0 eV. The ellipsometry spectra Ψ (relative amplitude change) and Δ (relative phase shift of the polarization) for the 10 nm Bi_2Se_3 film is shown in Figure 2(a). These data were modeled utilizing 3 Tauc-Lorentz oscillators. Table I summarizes the fitting results (see supplementary material for details about the model and fitting parameters). The substrate was modeled separately and then incorporated into the film + substrate model. The real and imaginary parts of the complex dielectric constant are shown in Fig. 2(b). Two peaks are observed, the strongest one at 2.0 eV and a shoulder at 1.4 eV (arrows in ε_2 data), which agrees very well with reports on MBE samples.[31] Band structure calculations can identify multiple candidates responsible for these transitions (both direct and indirect).[23,24] Even though the spectral range of our ellipsometry measurement is limited, empirical bandgaps can be inferred from the Tauc gaps (E_g) of the model oscillators (Table I). Ignoring the broad background oscillator (TL1), we find that the first Tauc gap is at 0.376 eV (E_g value for the TL2 oscillator), which is close to the gap value measured through absorption spectroscopy that is discussed next.

To perform the transmittance measurements, the Bi_2Se_3 samples were deposited on transparent quartz substrates. Two set of samples of thickness 2–10 QL were fabricated. One set was capped with a few nm of amorphous and transparent BN (bandgap > 5.5 eV) and the other set was left uncapped. This allowed us to protect the Bi_2Se_3 layer without affecting its visible and infrared transmittance. To

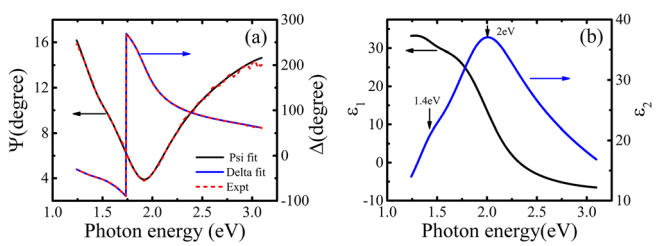

FIG. 2. (a) Experimental and fitted Psi (Ψ) and Delta (Δ) for the 10 QL Bi_2Se_3 sample on Si/SiO_2 for incident angle of 70°. (b) Extracted complex dielectric constants (ε_1,ε_2) of the film fitted in (a).

TABLE I. Fit parameters of Tauc-Lorentz oscillators.

	$\varepsilon_\infty = 1.44$			
Oscillator	Amp	E_n	C	E_g
TL_1	1.239	1.436	0.375	0.0001
TL_2	74.59	2.504	2.965	0.376
TL_3	30.075	1.999	0.88029	0.5221

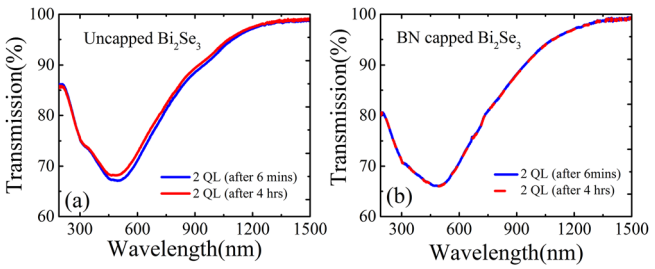

FIG. 3. Transmittance data of an uncapped (a) and BN-capped (b) 2QL Bi_2Se_3 film taken at different times after film deposition. The uncapped sample showed only little variation with time whereas the capped sample did not show any change at all.

ascertain the impact of oxidation and other surface changes on the optical characteristics of the films, we measured the transmittance of several capped and uncapped films at various times after deposition. In Figure 3, we show the data for the 2 QL film, which is the thinnest film studied, where presumably the oxidation effect, if any, should be the strongest. As expected, the uncapped sample demonstrated some change in its optical transmittance, but it is only a few percent and mostly in the high-energy range (500–900 nm). The observed change is less than 10% even after 7 days (data not shown), proving that the optical transmittance properties were not affected to any significant degree even at the 2 QL level. The BN capped sample did not show any change as evident from the perfect overlap of the data taken after 6 min and 4 h. We, therefore, infer that even though capping improves reliability, oxidation and other extrinsic effects do not dominate our optical measurements.[31] Encouraged by these developments, we proceeded to measure the bandgap on both types of samples.

In Figure 4(a), we plot the optical absorption values of the 2 and 6 QL films as calculated from transmittance (T) through the relation $\alpha = -(1/\text{thickness}) * \ln T$. Various optical features are observed that agree qualitatively with the 10 QL sample (Fig. 2 and Fig. S3 (supplementary material)). The most striking dissimilarity between the two films is the rigid blue shift in the 2 QL sample compared to the 6 QL data. This clearly indicates that the bulk bandgap of the two systems are different. The blue shift in the absorption data continues up to 3.5 eV, above which the optical characteristics overlap well.

To quantify the direct bandgaps accurately, we plot the $(\alpha E)^2$ vs the photon energy in Fig. 4(b). Though this method was developed to measure optical properties of semiconductors with parabolic bands, it has been extended to other systems. Using this method, the measured bandgap for the 2 QL film is found to be ~0.8 eV, whereas the value for the 6 QL film is ~0.5 eV. Extending this analysis to all films, we plot the bandgaps of all capped and uncapped samples. A strong increase in bandgap with decreasing thickness is observed regardless of capping. In particular, 2 and 3 QL films show the largest increase. We attribute this to finite size effects. The evidence for this is found in Zhang *et al.*[25] ARPES measurements show that the valence band maximum of a 2 QL film is about 0.3 eV deeper compared to the 6 QL film, which is exactly the bandgap difference we measure. Therefore, we infer that a bulk gap widening also occurs below 6 QL along with a surface gap opening. Very recent first-principles calculations also confirm this observation.[38]

Another important observation is that the bandgap values of thicker films (10 QL or more) are considerably larger than the reported bulk value by about 0.2 eV. We explain this as due to the Burstein-Moss (BM) effect, which is observed in semiconductors with high carrier concentrations ($>10^{18}\,cm^{-3}$).[39] In such cases, the Fermi level moves to the conduction band and results in an apparent increase in the bandgap due to Pauli blocking of occupied conduction band (CB) states. Preliminary Hall effect studies on our 10–30 QL films revealed a carrier concentration in excess of $10^{19}\,cm^{-3}$ which is typical of Bi_2Se_3.[40] Quite revealing is the ARPES and transport work by Analytis *et al.*[39] that showed that states up to 0.15 eV above the CB minimum are occupied in samples with concentrations above $10^{19}\,cm^{-3}$. This is consistent with increased bandgap values we report here. Therefore, it is clear that the BM effect is also producing an increase in the bandgap values in all films, apart from finite-size effects.

In conclusion, we have provided optical evidence for blue shift in Bi_2Se_3 thin films as we approach the two-dimensional limit. High-quality few-layer Bi_2Se_3 films were grown using magnetron sputtering, and their structural and optical properties were investigated using X-ray, Raman, spectroscopic ellipsometry, and transmittance spectroscopy. Up to 0.5 eV change in bandgap is observed, and most significantly below 6 QL. The effect is robust and is observed in both capped and uncapped films. We explain the increase through a combination of finite-size and Burstein-Moss effect. Overall, our data sheds more evidence into the scaling behavior of TI systems that can potentially have interesting

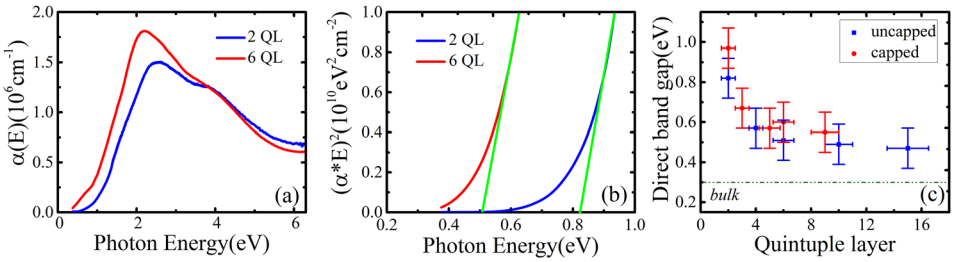

FIG. 4. (a) Optical absorption data of 2 and 6 QL Bi_2Se_3 films showing a blue shift with inverse thickness. (b) Direct-gap analysis of the data shown in (a). The blue shift is clearly quantified. (c) The direct bandgap for films of different thicknesses. Both capped and uncapped films follow the same trend of increasing bandgap with inverse thickness.

consequences in future nanoelectronic devices. The increase in bandgap can also be utilized in opto-electronic areas such as photodetector and solar cells.

See supplementary material for additional data and discussion on x-ray reflectivity/diffraction and ellipsometry measurements.

D.M. would like to acknowledge support from startup funds from Southern Illinois University (SIU), SIU Elevation research grant, and SIU Materials Technology Center. Raman measurements shown here were carried out at the Frederick Seitz Materials Research Laboratory Central Research Facilities, University of Illinois.

[1]M. Z. Hasan and C. L. Kane, "Colloquium: Topological insulators," Rev. Mod. Phys. **82**, 3045 (2010).
[2]X.-L. Qi and S.-C. Zhang, "Topological insulators and superconductors," Rev. Mod. Phys. **83**, 1057–1110 (2011).
[3]D. Hsieh, Y. Xia, D. Qian, L. Wray, J. H. Dil, F. Meier, J. Osterwalder, L. Patthey, J. G. Checkelsky, N. P. Ong, A. V. Fedrov, H. Lin, A. Bansil, D. Grauer, Y. S. Hor, R. J. Cava, and M. Z. Hasan, "A tunable topological insulator in the spin helical Dirac transport regime," Nature **460**, 1101 (2009).
[4]L. Fu, C. L. Kane, and E. J. Mele, "Topological insulators in three dimensions," Phys. Rev. Lett. **98**, 106803 (2007).
[5]F. Katmis, V. Lauter, F. S. Nogueira, B. A. Assaf, M. E. Jamer, P. Wei, B. Satpati, J. W. Freeland, I. Eremin, D. Heiman, P. Jarillo-Herrero, and J. S. Moodera, "A high-temperature ferromagnetic topological insulating phase by proximity coupling," Nature **533**, 513–516 (2016).
[6]G. J. Ferreira and D. Loss, "Magnetically defined qubits on 3D topological insulators," Phys. Rev. Lett **111**, 106802 (2013).
[7]A. V. Kitaev, "Fault-tolerant quantum computation by anyons," Ann. Phys. **303**, 2–30 (2003).
[8]C. Nayak, S. H. Simon, A. Stern, M. Freedman, and S. Das Sarma, "Non-Abelian anyons and topological quantum computation," Rev. Mod. Phys. **80**, 1083 (2008).
[9]A. R. Mellnik, J. S. Lee, A. Richardella, J. L. Grab, P. J. Mintun, M. H. Fischer, A. Vaezi, A. Manchon, E.-A. Kim, N. Samarth, and D. C. Ralph, "Spin-transfer torque generated by a topological insulator," Nature **511**, 449–451 (2014).
[10]A. Akhmerov, J. Nilsson, and C. Beenakker, "Electrically detected interferometry of Majorana fermions in a topological insulator," Phys. Rev. Lett. **102**, 216404 (2009).
[11]Y. Xia, D. Qian, D. Hsieh, L. Wray, A. Pal, H. Lin, A. Bansil, D. Grauer, Y. S. Hor, R. J. Cava, and M. Z. Hasan, "Observation of a large-gap topological-insulator class with a single Dirac cone on the surface," Nat. Phys. **5**, 398–402 (2009).
[12]H. Zhang, C.-X. Liu, X.-L. Qi, X. Dai, Z. Fang, and S.-C. Zhang, "Topological insulators in Bi_2Se_3, Bi_2Te_3, and Sb_2Te_3 with a single Dirac cone on the surface," Nat. Phys. **5**, 438–442 (2009).
[13]P. Roushan, J. Seo, C. V. Parker, Y. S. Hor, D. Hsieh, D. Qian, A. Richardella, M. Z. Hasan, R. J. Cava, and A. Yazdani, "Topological surface states protected from backscattering by chiral spin texture," Nature **460**, 1106 (2009).
[14]W. Zhang, R. Yu, H.-J. Zhang, X. Dai, and Z. Fang, "First-principles studies of the three-dimensional strong topological insulators Bi_2Te_3, Bi_2Se_3, and Sb_2Te_3," New J. Phys. **12**, 065013 (2010).
[15]M.-X. Wang, C. Liu, J.-P. Xu, F. Yang, L. Miao, M.-Y. Yao, C. L. Gao, C. Shen, X. Ma, X. Chen, Z.-A. Xu, Y. Liu, S.-C. Zhang, D. Qian, J.-F. Jia, and Q.-K. Xue, "The Coexistence of superconductivity and topological order in the Bi_2Se_3 thin films," Science **336**, 52–55 (2012).
[16]L. Fu and C. L. Kane, "Superconducting proximity effect and Majorana fermions at the surface of a topological insulator," Phys. Rev. Lett. **100**, 096407 (2008).
[17]C. Chang, J. Zhang, X. Feng, J. Shen, Z. Zhang, M. Guo, K. Li, Y. Ou, P. Wei, L. Wang, Z. Ji, Y. Feng, S. Ji, X. Chen, J. Jia, X. Dai, Z. Fang, S. ZHang, K. He, Y. Wang, L. Lu, X. Ma, and Q. Xue, "Experimental observation of the quantum anomalous Hall effect in a magnetic topological insulator," Science **340**, 167 (2013).
[18]J. G. Checkelsky, R. Yoshimi, A. Tsukazaki, K. S. Takahashi, Y. Kozuka, J. Falson, M. Kawasaki, and Y. Tokura, "Trajectory of the anomalous Hall effect towards the quantized state in a ferromagnetic topological insulator," Nat. Phys. **10**, 731 (2014).
[19]R. Yu, W. Zhang, H.-J. Zhang, S.-C. Zhang, X. Dai, and Z. Fang, "Quantized anomalous Hall effect in magnetic topological insulators," Science **329**, 61 (2010).
[20]J. Linder, T. Yokoyama, and A. Subdo, "Anomalous finite size effects on surface states in the topological insulator Bi_2Se_3," Phys. Rev. B **80**, 205401 (2009).
[21]C.-X. Liu, H. Zhang, B. Yan, X.-L. Qi, T. Frauenheim, X. Dai, Z. Fang, and S.-C. Zhang, "Oscillatory crossover from two-dimensional to three-dimensional topological insulators," Phys. Rev. B **81**, 041307(R) (2010).
[22]H.-Z. Lu, W.-Y. Shan, W. Yao, Q. Niu, and S.-Q. Shen, "Massive dirac fermions and spin physics in an ultrathin film of topological insulator," Phys. Rev. B **81**, 115407 (2010).
[23]W. Liu, X. Peng, X. Wei, H. Yang, G. M. Stocks, and J. Zhong, "Surface and substrate induced effects on thin films of the topological insulators Bi_2Se_3 and Bi_2Te_3," Phys. Rev. B **87**, 205315 (2013).
[24]J. Betancourt, S. Li, X. Dang, J. D. Burton, E. Y. Tsymbal, and J. P. Velev, "Complex band structure of topological insulator Bi_2Se_3," J. Phys.: Condens. Matter **28**, 395501 (2016).
[25]Y. Zhang, K. He, C.-Z. Chang, C.-L. Song, L.-L. Wang, X. Chen, J.-F. Jia, Z. Fang, X. Dai, W.-Y. Shan, S.-Q. Shen, Q. Niu, X.-L. Qi, S.-C. Zhang, X.-C. Ma, and Q.-K. Xue, "Crossover of the three-dimensional topological insulator Bi_2Se_3 to the two-dimensional limit," Nat. Phys. **6**, 584 (2010).
[26]Y. Sakamoto, T. Hirahara, H. Miyazaki, S.-I. Kimura, and S. Hasegawa, "Spectroscopic evidence of a topological quantum phase transition in ultrathin Bi_2Se_3 films," Phys. Rev. B **81**, 165432 (2010).
[27]Q. Yang, M. Dolev, L. Zhang, J. Zhao, A. D. Fried, E. Schemm, M. Liu, A. Palevski, A. F. Marshall, S. H. Risbud, and A. Kapitulnik, "Emerging weak localization effects on a topological insulator–insulating ferromagnet (Bi_2Se_3-Eus) interface," Phys. Rev. B **88**, 081407(R) (2013).
[28]H. Wang, H. Liu, C.-Z. Chang, H. Zuo, Y. Zhao, Y. Sun, Z. Xia, K. He, X. Ma, X. C. Xie, Q-k. Xue, and J. Wang, "Crossover between weak antilocalization and weak localization of bulk states in ultrathin Bi_2Se_3 films," Sci. Rep. **4**, 5817 (2014).
[29]A. Vargas, S. Basak, F. Liu, B. Wang, E. Panaitescu, H. Lin, R. Markiewicz, A. Bansil, and S. Kar, "The changing colors of a quantum-confined topological insulator," ACS Nano **8**, 1222–1230 (2014).
[30]K. W. Post, B. C. Chapler, L. He, X. Kou, K. L. Wang, and D. N. Basov, "Thickness-dependent bulk electronic properties in Bi_2Se_3 thin films revealed by infrared spectroscopy," Phys. Rev. B **88**, 075121 (2013).
[31]M. Eddrief, F. Vidal, and B. Gallas, "Optical properties of Bi_2Se_3: From bulk to ultrathin films," J. Phys. D **49**, 505304 (2016).
[32]J. Son, K. Banerjee, M. Brahlek, N. Koirala, S.-K. Lee, J.-H. Ahn, S. O. Oh, and H. Yang, "Conductance modulation in topological insulator Bi_2Se_3 thin films with ionic liquid," Appl. Phys. Lett. **103**, 213114 (2013).
[33]H. Peng, W. Dang, J. Cao, Y. Chen, D. Wu, W. Zheng, H. Li, Z.-X. Shen, and Z. Liu, "Topological insulator nanostructures for near-infrared transparent flexible electrodes," Nat. Chem. **4**, 281–286 (2012).
[34]H. Samassekou, A. Alkabsh, M. Wasala, M. Eaton, A. Walker, O. Pitkänen, K. Kordas, S. Talapatra, T. Jayasekara, and D. Mazumdar, "Viable route towards large-area two dimensional MoS_2 using magnetron sputtering," 2D Mater. **4**, 021002 (2017).
[35]M. Bjorck and G. Andersson, "GenX: An extensible X-ray reflectivity refinement program utilizing differential evolution," J. Appl. Crystallogr. **40**, 1174–1178 (2007).
[36]L. G. Parratt, "Surface studies of solids by total reflection of X-rays," Phys. Rev. **95**, 359 (1954).
[37]J. Zhang, Z. Peng, A. Soni, Y. Zhao, Y. Xiong, B. Peng, J. Wang, M. S. Dresselhaus, and Q. Xiong, "Raman spectroscopy of few-quintuple layer topological insulator Bi_2Se_3 nanoplatelets," Nano Lett. **11**, 2407 (2011).
[38]J. Sun and D. J. Singh, "Using gapped topological surface states of Bi_2Se_3 films in a field effect transistor," J. Appl. Phys. **121**, 064301 (2017).
[39]E. Burstein, "Anomalous optical absorption limit in InSb," Phys. Rev. B **93**, 632 (1954).
[40]J. G. Analytis, J.-H. Chu, Y. Chen, F. Corredor, R. D. McDonald, Z. X. Shen, and I. R. Fisher, "Bulk Fermi surface coexistence with Dirac surface state in Bi_2Se_3: A comparison of photoemission and Shubnikov–de Haas measurements," Phys. Rev. B **81**, 205407 (2010).